TOPOLOGICALLY ROBUST RECONSTRUCTION OF A 3D OBJECT WITH ORGANIZED MESHING

Junta Doi, Wataru Sato
Department of Computer Science, Chiba Institute of Technology, Narashino, Japan

Keywords: 3D reconstruction, Polygonal scanning, Organized meshing, Quadrilateral mesh, Hexagonal mesh, Matrix format data structure, 3D shape modification, Topology conserved reconstruction.

Abstract: This paper proposes a practical, topologically robust and ranging error resistive shape modeling procedure that approximates a real 3D object with the matrix-formatted organized meshing for the 3D shape processing. A geometric model with desired meshing, not limited to triangular one, but also quadrilateral, hexagonal or n-gonal mesh, is directly reconstructed based on a solid modeling approach. The radial distance of each scanning point from the axis of the cylindrical coordinates is measured by laser triangulation. The angular and vertical positions of the laser beam are two other coordinate values of the scanning. A face array listing (topology), which defines the vertex (sampling point) connectivity and the shape of the mesh, is assigned to meet the desired meshing. Stable meshing, and hence, an accurate approximation, free from the shape ambiguity unavoidable in the widely used ICP (Iterative Closest Point) modeling, is then accomplished. This proposal allows a practical and versatile reconstruction and the successive 3D shape modification.

1 INTRODUCTION

The problem of shape reconstruction has been the focus of research across many fields because of its wide applications. Attempts to measure the shape of objects and to construct geometric models have a long history. There are a great number of books (Mantyla, 1988, Hartley et al., 2000, and Forsyth et al., 2003), review articles (Chen et al., 2000, Scott et al., 2003, and Blais, 2004), papers (Besel, 1992, Turk et al., 1994, Levoy et al., 2000, Rusinkiewicz et al., 2001, Godin et al., 2002, Pauly et al., 2003, and Dey et al., 2004), and products (Simple3D, 2005) dealing with the problems.

This study is to provide technology that would reconstruct the objects, such as, cultural heritage artifacts and reliefs, accurately and precisely as they are in a usually noisy environment. A 3D shape processing for reuse of the geometric models is our purpose of the proposal.

Surface models with unorganized triangular meshes have been built based on the ICP algorithm from the scanned cloud points obtained by, for instance, triangulation scanners so far. A great deal of research efforts has been made on the problem. The ICP algorithm is widely used and well proven in some applications; however, it is ranging-noise sensitive and hence shape-ambiguous, and complicated for constructing a fully automated system.

In general, the presence of noise (the ranging noise or triangulation error) is typical for the scanning process. Retrieving surface topology from surface geometry as the algorithm is not easy, when the ranging noise is unavoidable. Many attempts have been made to overcome the problem; however, there is no known algorithm that has theoretical guarantees, without assumptions, for surface reconstruction in the presence of noise (Dey et al., 2004).

The triangulation error arises mostly from the oblique reflection of the incident laser beam on the local surface. To reduce the error, a large object model with rather flat surfaces is to be employed. The surface polishing is most effective for an error-free and reliable triangulation. These measures are, however, not applicable to most of the objects that should be treated as they are.

Contrary to the widely used procedures, this paper proposes an approach such that the surface topology is first assigned and a geometric model with a solid model format with the desired meshing is directly generated.

In other words, the method involves a prototypical model (e.g., the unit cylinder in Fig. 1) being first prepared by considering the shape of the object

Doi J. and Sato W. (2005).
TOPOLOGICALLY ROBUST RECONSTRUCTION OF A 3D OBJECT WITH ORGANIZED MESHING.
In *Proceedings of the Second International Conference on Informatics in Control, Automation and Robotics - Robotics and Automation*, pages 154-159
DOI: 10.5220/0001179001540159

and then modifying every mesh point to reflect the geometric shape of the object. This is "topology is first and then geometry" not that "geometry first and then topology" as the IPC modeling.

This model is called "B-reps (Boundary representations)" which describes a 3D object as a set of surfaces that separate the object interior from the environment and is a polygon mesh approximation of a curved object surface.

Usually, irregular triangular meshes, generated, for instance, by the algorithm, are re-sampled into regular meshes when required. However, point-locatable nature and accuracy are lost in the re-meshing process. Very many scientific efforts are focused on the unorganized meshing, however, to our knowledge; few published works that can be related to this proposal of organized meshing have been presented.

During morphing or warping, which is a fundamental operation in computer graphics, the initially constructed model is deformed into another model. Usually it is computer-graphics-based and operation is applied to unorganized triangular meshes, which are not surface-point-position- locatable. Our shape deformation is applied to the organized and point-locatable model, originated from the modeling procedure, using intuitive matrix-type operators enabling the quantitative shape modification, evaluation and CAD compatibilities.

Laser triangulation sensors using the spot and stripe projections are used for the examples in this paper, but the measurement procedure is general and not limited to these. As a modeling/rendering system, we prepared some solid model interfaces for popular computer graphics or computer-aided design systems.

2 SOLID MODELING

In the illustration of a solid model data structure in Fig. 1, a pentahedral volume element, in which the peripheral surface is covered with a rectangular mesh, small enough to approximate the curved object surface, is to be measured to approximate the object shape. A quadrilateral mesh Sa, consisting of four surface points, a, b, c and d, is one of the sampling points on the object surface. Points A, B, C and D are mesh points consisting of a rectangular mesh SA on the unit cylinder surface. The rectangu- lar mesh SA is a perspective projection of the quadrilateral mesh Sa to the unit cylinder surface, and vice versa. Each radial distance of the object surface point from the axis of rotation (z-axis), for instance, "r_a, r_b, ⋯" is sequentially measured. We call this type

Table 1: Vertex array listings (geometry) for the rectangular surface mesh SA (left, on the unit cylinder surface) and the quadrilateral Sa (right, on the object surface) in Fig. 1.

Vertex	r	θ	z	Vertex	r	θ	z
SA: A	1	0	z_1	Sa: a	r_a	0	z_1
B	1	θ	z_1	b	r_b	θ	z_1
C	1	θ	z_2	c	r_c	θ	z_2
D	1	0	z_2	d	r_d	0	z_2

Table 2: Face array listings (topology) for the mesh SA (on the unit cylinder) and Sa (on the object surface) in Fig.1.

Face	1	2	3	4	Face	1	2	3	4
SA(u)	B	C	D	A	Sa(o)	b	c	d	a

Table 3: Vertex array listings (geometry) for the quadrilateral mesh SA (left, on the object surface) and the rectangular mesh Sa (right, on the unit cylinder surface) in Fig. 2.

Vertex	r	θ	z	Vertex	r	θ	z
SA: A	r_a	0	z_1	Sa: a	1	0	z_1
B	r_b	θ	z_1	b	1	θ	z_1
C	r_c	θ	z_2	c	1	θ	z_2
D	r_d	0	z_2	d	1	0	z_2

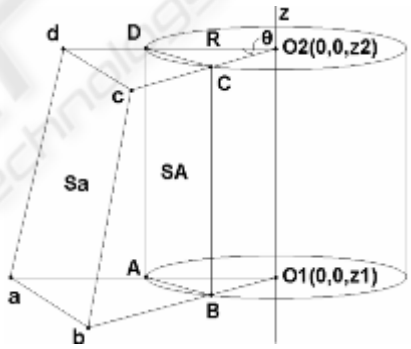

Figure 1: The mesh structure of a solid model cylinder for scanning of an object on the axis (object-modeling mode).

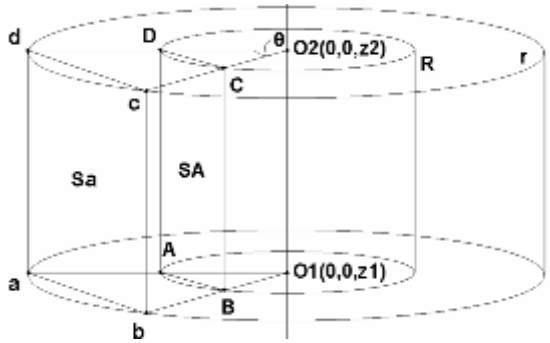

Figure 2: The mesh structure of a solid model concentric cylinder for the outer scene scanning (scene-modeling mode). The outer cylinder with a radius "r" is a cut-off limit of the ranging sensor. A quadrilateral mesh "SA" is on the object surface. "Sa" is a rectangular mesh on the cut-off cylinder.

of modeling the "object-modeling mode."

A vertex array listing, which is called "geometry" and represents the geometric coordinate values in 3D space is shown in Table 1. The face (mesh) array listings for the Sa and SA are shown in Table 2. Other four comprising surfaces of the wedge shaped pentahedral volume element are similarly defined (Tables not shown). The listing is called "topology" and defines the shape of the face (number of vertices or edges) and also defines the listing sequence of the vertices or connectivity. The listing sequence of the vertices in the face list defines the normal vector direction of the face and determines on which side of the face the solid part of the object exists. This mesh is directly compatible with that used in the BEM (Boundary Element Method).

As shown in Fig. 1 and Table 2, the variation in the radial distance (depth) of a, in principle, has no effect on the connectivity array of the face, if point a locates along the radial line segment O1-a or O1-A. This relation is also valid for the other points b, c, and d as well. Therefore, the connectivity array of the mesh is conserved if the four points similarly locate along each radial line. The vertex connectivity of Sa is the same as that on the unit cylinder, SA as shown in Fig. 1 and Table 2. This means that the face array listing assigned for the unit surface SA is valid for the object surface Sa. N-gonal meshes are similarly constructed (Doi et al., 2004).

When the triangulation sensor is set at the axis of the coordinate and rotates to measure the distance to the outside scene, the solid modeling is as shown in Table 3 and Fig. 2, where the object surface is SA and the mesh is defined on a cut-off circle or a unit circle. A Boolean subtraction of a pentahedron including SA from that including Sa results in a hexahedral element in a solid model of the scene. We call this the "scene-modeling mode." The modeling procedure is similar to the "object- modeling mode."

Our mesh shape is arbitrary. In this procedure, it is triangular, quadrilateral, hexagonal or even n-gonal, if required for a more reduced number of meshes. Figure 3 shows a hexagonal mesh. Our hexagonal meshing is based on a 1/2 interlacing scan as shown in the figure, similar to that of the NTSC video format. A hexagon can be broken down into six small triangular meshes, one is, for instance ABG, or two trapezoids, for instance, ABCF, or three rhomboidal meshes, for instance, GDEF. The combination of hexagonal, rhomboidal and triangular meshes is useful to efficiently cover the variously curved object surfaces with a reduced number of meshes.

Our data format is a raster scan type or a matrix format according to the above procedure as described

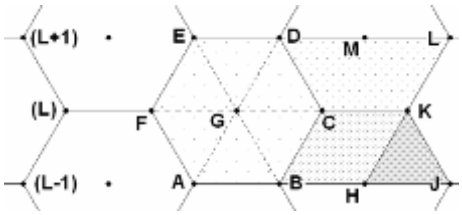

Figure 3: An example of a hexagonal mesh ABCDEF, which is consisted of two trapezoidal ABCF and DEFC, three rhomboids, such as, BCDG, and six triangles, such as, ABG. Three horizontal scan lines, (L-1), (L) and (L+1) make a hexagonal mesh. A sequential scan makes a rectangular mesh.

Figure 4: Photograph of the object sculpture head (Niobe) (top) and the shaded image of the object-modeled result (bottom). Angular scanning step is 0.4 degrees in the frontal region (rear; 0.8 degrees)and vertical step is 0.45 mm

Figure 5: Photograph of the object sculpture shown above (left) and the shaded image of the modeled result (right).

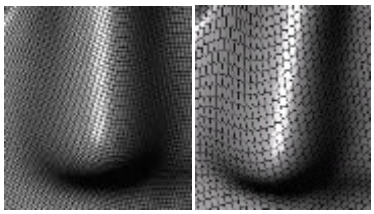

Figure 6: Shaded images of the modeled nose part of the sculpture (Niobe). Modeled result with overlaid quadrilateral meshes (left) and hexagonal meshes (right).

above and it is as follows.

$$\mathbf{r} = [\mathbf{r}_{ij}] = \begin{bmatrix} \mathbf{r}_{11} & \mathbf{r}_{12} & \cdots & \mathbf{r}_{1m} \\ \mathbf{r}_{21} & \mathbf{r}_{22} & \cdots & \mathbf{r}_{2m} \\ \vdots & \vdots & \ddots & \vdots \\ \mathbf{r}_{n1} & \mathbf{r}_{n2} & \cdots & \mathbf{r}_{nm} \end{bmatrix} \quad (1)$$

An element $\mathbf{r}_{ij}$ represents the radial distance of a sampled surface point at the angular position "j" and at the vertical position "i" in the scanning This matrix can easily locate an arbitrary point on the object only by specifying "i" and "**j**."

An object such as a sculpture is placed on a turn-table which is driven by a geared pulse motor with angular resolution of 0.02 degrees. This means that the horizontal resolution is 0.015 mm at the radius of 43 mm and there are a maximum of 18,000 horizontal meshes in one 360 degree turn. The translational resolution of the vertical slider, which is also driven by a geared pulse motor, is 0.015 mm with a maximum stroke of 500 mm. There are 33,333 vertical meshes at maximum in the full stroke. Therefore, the maximum number of the quadrilateral meshes is 600 million. In our 600 mega-cloud-points, each mesh contains additional RGB color information.

In the demonstrations hereafter, however, rendering points are reduced to 1/10 in horizontal, 1/10 in vertical and 1/100 of the scanned points in total, which is about 6 mega-points, for a file size reduction and quick rendering.

A triangulation sensor with a 690-nm diode laser was installed on the vertical slider. The laser power is 15 mW and the spot size on the object surface is about 0.3 mm in diameter. A sensing range from 250 mm to 750 mm is produced here with a resolution of 0.01 mm at best. A laser stripe projector with a line width of 1 mm was also used. In the proposal, the measurement procedure is general and not limited to this type of sensing. As a modeling/rendering system, we prepared solid model interfaces for the popular 3D computer graphics and computer-aided design systems.

3 RESULTS AND DISCUSSION

The desired meshing, for instance, the rectangular mesh SA is first assigned for the sampling point connection and then the vertex array listing is continuously updated. Our procedure results in the "B-reps" model, which describes a 3D object as a set of the organized meshes.

Photographs of a plaster sculpture (Niobe) are in Figs. 4 (top) and 5 (left). The object-modeled result is shown in Figs. 4 (bottom) and 5 (right). The result is estimated to be accurate in an extent of the resolution

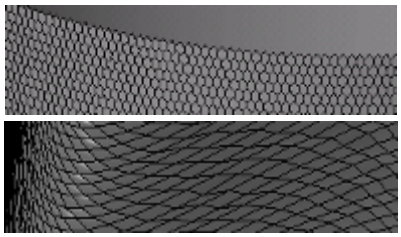

Figure 7: Hexagonal meshes on the unit cylinder in Fig. 2 (top) and rhomboidal meshes made from the hexagons.

Figure 8: Photographs of an object stone sculpture (Cleopatra). The face is 60 mm high and partly black painted.

Figure 9. Shaded images of the modeled results. A frontal image (left) and a side image (center), a side image of the shape modified long nose (right). A 20% of the radial distance from the axis around the top of the nose is expanded.

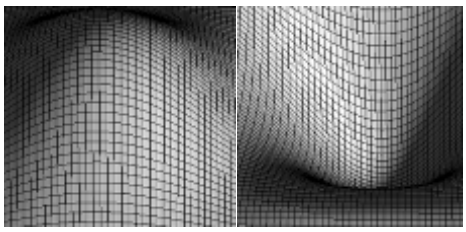

Figure 10: Two examples of 128x128 (overlaid wire-frame representation in 64x64) shape-to-shape (depth-to-depth) transformation operators. The left figure is positive and the right negative. The parameter distribution is sinusoidal in horizontal (peripheral) and vertical directions. They are configured similarly to the 2D image processing operators.

of 0.015 mm. in all three directions.

Figure 6 (left) is an example of the modeled result with quadrilateral mesh. Here, triangulation is based on the laser light stripe projection. It is not as accurate as the laser spot triangulation. An example of the modeled result with hexagonal meshes is shown in Fig 6 (right). An example of the hexagonal meshes on the unit cylinder is illustrated in Fig. 7 (top) and an example of the rhomboidal meshes from the hexagonal meshes is in Fig. 7 (bottom).

Photographs of a stone sculpture (Cleopatra) are shown in Fig. 8. Some ranging noises are observed in the modeled result (Data not shown). In spite of the noises, the surrounding mesh points are observed as unaffected, showing that each noise is standing alone and isolated, and the topology is robust and unchanged as expected from the modeling procedure explained previously. The smoothed model is shown in Figs. 9 (left) and 9 (center).

A 3x3 or 5x5 depth-to-depth transformation operator, which is similar to a two-dimensional smoothing operator, is sequentially applied to the matrix-type output data. If the noise is detected, the point is replaced with the surrounding data.

The matrix type data is convenient and essential for modifying a local shape when locating the target position. In Fig. 8 (right), the nose of the statue is modified in shape and size. Referring to the initial model in Fig. 8 (center), the modifications are three-dimensionally applied and evaluated. This is supposing the restoration of a broken artifact, for instance, the addition of a lost nose, or for virtual training of, for instance, cosmetic surgery. In the figure, a 128x128 depth-to-depth transformation operator, shown in Fig. 10 (left), similar to the image intensifying operator, is applied.

The modeled result may be used again as an operator. Two examples are shown in Fig. 11. One is a rectangular matrix in the cylindrical surface and the other is a recursive operator generated by this modeling procedure for use in convolution or 3D shape fusion. This is not the so called morphing operation but the quantitative 3D shape operation with CAD compatibility.

A combination of variously shaped polygons is used for efficient meshing and watermarking as shown in Fig. 12. Figure 13 (left) is a photograph of the backside of a scarab beetle stone and the modeled result (right). It is about 100 mm long and 70 mm wide. An underside image of the stone engraved with hieroglyphs is shown in Fig. 14 (left) and the shaded image of the modeled result is in Fig 14 (right). It is an example of the scene-modeling mode. The modeling is similar to a reconstruction of a relief. In the comparison, a pictorial image is not the same as the modeled depth image. It may be concluded that the depth image is well reproduced in an extent of

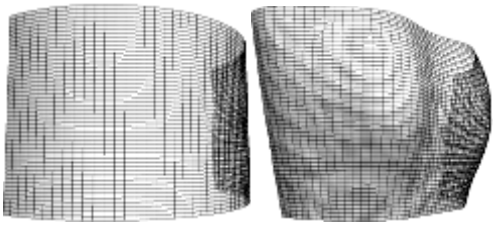

Figure 11: A bread arc-board instead of a planar board, such as Eq. (1) (left), and a customized 3D depth-to-depth transformation operator, which may be a thus reconstructed model of a real object based on triangulation. This 3D shape replaces a part of the initial shape. Convolution of the reconstructed model operator fuses two shapes together.

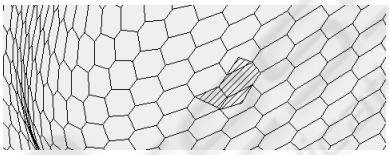

Figure 12: An example of polygonal surface comprising of hexagonal, trapezoidal, rhomboidal and triangular meshes. A combination of the variously shaped polygons serves the efficient surface approximation with a reduced number of meshes and also embedded watermarking.

Figure 13: Backside photograph of the object stone sculpture (top) and the shaded image of the modeled result (bottom)

Figure 14: Underside photograph of the scarab beetle stone engraved with hieroglyphs (left) and the shaded image of the scene-modeled result. The pictorial image is similar but not the same as the modeled depth image.

the 0.015mm resolution.

The modeling accuracy depends on the rotational and translational positioning, and distance-sensing. The mal-aligned positioning results in a shape distortion, but still generates topologically stable models.

4 CONCLUDING REMARKS

A simple, automatic, geometrically accurate, topologically stable, robust and noise-resistive object modeling, with matrix format meshes, to be followed by quantitative 3D shape processing, is proposed.

Most of the reconstruction procedures from the unorganized set of points are based on the principle: "retrieving surface topology from surface geometry." In general, "retrieving topology from geometry," where appropriate distance-based criteria are used for the modeling, is not easy especially in the presence of noise even in the dense data-sets. Our topology, on the contrary, is not dependent on geometry. In our procedure, "topology is first assigned in the scanning stage and geometry follows." The noise problem is inherent in the triangulation scanning, which is fatal in the ICP algorithm due to point-connection (topology) ambiguities caused by the problem, is solved using the matrix format smoothing operators for practical usage in the exchange for some spatial resolution reduction.

The matrix format of the modeled data is intuitive and easy to apply to the quantitative shape modification using the various matrix type 3D shape modification operators, which recursively include thus modeled results with the same matrix format. The 3D shape models are fused together by convolution. The data format is compatible with that of the BEM/FEM. The desired meshing, not limited to triangular, but quadrilateral, hexagonal, and even n-gonal meshes, is possible in the same way.

A Boolean operation with multi-directional modeling is currently underway. We expect considerable utility in the practical approximate modeling and 3D shape processing.

REFERENCES

Blais, F., 2004, Review of 20 Years of Range Sensor Development, *Journal of Electronic Imaging*, 13 (1), 231-240.

Boissonnat, J., 1984, Geometric Structures for Three-Dimensional Shape Representation, *ACM Transactions on Graphics*, 3 (4), 266-286.

Chen, F., Brown, G., Song, M., 2000, Overview of Three-Dimensional Shape Measurement Using Optical Methods, *Optical Engineering*, 39 (1), 10-22.

Dey, T., Goswami, S., 2004, Provable Surface Reconstruction from Noisy Samples, Annual Symposium on Computational Geometry, In *Proceedings of 20th Annual Symposium on Computational Geometry*, 330-339.

Doi, J., Sato, W., Miyamoto, Y., Ando, S., Yamanaka, M., 2004, Reuse of a Geometric Model for Shape Approximation, In *Proceedings of 2004 IEEE International Conference on Information Reuse and Integration (IRI 2004)*, 174- 179.

Forsyth, D., Ponce, J., 2003, *Computer Vision - A modern Approach*, Prentice Hall, New Jersey.

Godin, G., Beraldin, J., Taylor, J., Cournoyer, L., El-Hakim, S., Baribeau, R., Blais, F., Boulanger, P., Domey, J., Picard, M., Active Optical 3D Imaging for Heritage Applications *IEEE Computer Graphics and Applications,* 22, 24-36, 2002.

Hartley, H.,. Zisserman, A., 2000, *Multiple View Geometry in Computer Vision*, Cambridge Univ. Press, Cambridge, UK..

Levoy, M., Pulli, K., Curless, B., Rusinkiewicz, S., Koller, D., Pereira, L., Ginzton, M., Anderson, S., Davis, J., Ginsberg, J., Shade, J., Fulk, D., The Digital Michelangelo Project; 3D Scanning of Large Statues, In *Proceedings of Siggraph 2000*, 131-144, 2000.

Mantyla, M., 1988, *An Introduction to Solid Modeling*, Computer Science Press, Rockville, Maryland.

Paul J., Besl, P., McKay, D., 1992, A Method for Registration of 3-D Shapes, *IEEE Transactions on Pattern Analysis and Machine Intelligence*, 14 (2), 239-256.

Pauly, M., Keiser, R., Kobbelt, L., Gross, M., 2003, Shape Modeling with Point-Sampled Geometry, *ACM Transactions on Graphics (TOG), 22 (3), Special issue: Proceedings of ACM SIGGRAPH*, 641-650.

Rusinkiewicz, S.,. Levoy, M., 2001, Efficient Variants of the ICP Algorithm, In *Proceedings of the 3rd International Conference on 3-D Digital Imaging and Modeling (3DIM '01)*, 145-152.

Scott, W., Roth, G., Rivest, J., 2003, View Planning for Automated Three-Dimensional Object Reconstruction and Inspection, *ACM Computing Surveys*, 35(1), 64-96.

Simple3D, 2005, 3D Scanners, Digitizers, and Software for Making 3D Models and 3D Measurements, http://www. simple3d.com/

Turk, G., Levoy, M., 1994, Zippered Polygon Meshes from Range Images, In *Proceedings of SIGGRAPH 1994*, 311- 318.